Crystal structure and electronic properties of the new compound U$_3$Fe$_4$Ge$_4$

D. Berthebaud[1], O. Tougait[1]*, M. Potel[1], E.B. Lopes[2], J.C. Waerenborgh[2], A.P. Gonçalves[2]

and H. Noël[1]

[1] Laboratoire de Chimie du Solide et de Matériaux. UMR CNRS 6226, Université de Rennes 1, Avenue de Général Leclerc, 35042 Rennes, France

[2] Departamento. de Química, Instituto Tecnológico e Nuclear/CFMC-UL, P-2686-953 Sacavém, Portugal

* Corresponding author :   Dr. Olivier TOUGAIT
                            Université de Rennes1
                            CSM, UMR CNRS 6226
                            263 avenue du Général Leclerc,
                            35042 Rennes, France
                            Tel : ++ 33 2 23 23 57 40
                            Fax : ++ 33 2 23 23 67 99
                            Email: tougait@univ-rennes1.fr

Abstract.

The new ternary compound $U_3Fe_4Ge_4$ was prepared by melting the pure metals in the stoichiometric ratio. An ingot of large scale domain was obtained by decreasing the temperature from the liquid to 1000°C over 4 hours. Single crystal X-ray diffraction revealed that $U_3Fe_4Ge_4$ crystallizes with the $Gd_3Cu_4Ge_4$ type of structure, in the orthorhombic space group, *Immm* (n° 71), Z = 2, with unit-cell parameters at room temperature of, a=4.090(5)Å, b =6.639(5)Å and c=13.702(5)Å. The crystal structure is characterized by two U, one Fe and two Ge independent crystallographic positions and can be described as resulting from the condensation by face-sharing and edge-sharing of U(1)Ge6 octahedrons, U(2)Ge6 trigonal prisms and Fe(1)Ge4 tetrahedrons. The electronic properties of this new compound were investigated by means of electrical resistivity, thermopower, dc-susceptibility and Mossbauer spectroscopy. The transport properties of $U_3Fe_4Ge_4$ appears to be govern, in the temperature domain investigated (1.5 – 300K), by two competing mechanism of electrical conductivity that alternatively dominates as a function of the temperature. It yields a compound, best described as a semi-metal, with extremely low value of the Seebeck coefficient. The magnetic susceptibility also reflects a change in the electronic properties, with a high temperature domain governs by localized effective moments whereas at low temperature a significant reduction of the magnetic moments is observed. $U_3Fe_4Ge_4$ undergoes to a ferromagnetic ordering below T_C = 17(1) K. The low temperature (4.2K) ^{57}Fe Mossbauer spectra can be well fitted using a model with Fe atoms in a paramagnetic state, suggesting that the magnetic ordering originates from the U atoms only.

Keywords; Actinide, Uranium, Iron, Heavy Fermion, Magnetic Susceptibility, Electrical Resistivity, Thermopower, Mossbauer spectroscopy.

1. **Introduction.**

During the past four decades, U-based intermetallics always have been revealed to be a continuous source of exceptional materials for the study of unusual physical properties. They exhibit a wide variety of electronic phenomena including the unique example of coexistence of superconductivity and ferromagnetism at ambient pressure, as demonstrated with the two compounds URhGe [1] and UCoGe [2].

The large diversity in the physical properties of uranium compounds is mainly due to the particular nature of the 5f states. Their energy and spatial extension are responsible for a considerable hybridization of the 5f electrons with the valence states of the neighboring atoms in the crystal lattice. In this respect, the intermetallic systems combining U and Fe have to be considered of considerable importance due to the high degree of delocalization of the U 5f electrons that directly hybridize with the Fe 3d electrons [3]. As a consequence of the strong hybridization between U 5f and Fe 3d wave functions, is the reduction up to the cancellation of the magnetic moment borne by both the uranium and the iron atoms, as it is well illustrated for the ternary phases of the U-Fe-Si system, which exhibit electronic properties mainly govern by itinerant electrons [4 and ref. therein]. Therefore, in ternary systems involving U, Fe and a p bloc element, a gain of localization of the 5f electrons should be achieved by decreasing the strong interactions between the 5f and 3d wave functions and increasing the interactions between the 5f and np wave functions. Such an enlargement of the overlap of the 5f and np wave function should be attained by substituting Si (2p outer wave-functions) by a heavier p-element such as Ge (3p outer wave function).

This present work is a part of the large investigation of the U-Fe-Ge ternary system, undertook in the whole concentration range. In this ternary system, the previously reported ternary intermetallic compounds were UFeGe (*P2₁/m*, type UFeGe below 500K, and *Pnma*, type TiNiSi above 500K) [5], UFe₂Ge₂ (*I4/mmm*, type ThCr₂Si₂) [6], UFe₆Ge₆ (*P6/mmm*, type

YbCo$_6$Ge$_6$) [7], and the solid solution U$_2$Fe$_{17-x}$Ge$_x$ with 2<x<3 (*P6$_3$/mmc*, type Th$_2$Ni$_{17}$) [8], in addition to the recently reported U$_2$Fe$_3$Ge (*P6$_3$/mmc*, type MgZn$_2$) [9, 10].

U$_3$Fe$_4$Ge$_4$ is a new intermetallic compound found during this systematic investigation. We present here, the details about its crystal structure and electronic properties, including transport properties (electrical resistivity and thermopower) and magnetic behaviour (dc-magnetisation and Mössbauer spectroscopy) revealing at low temperature itinerant ferromagnetism.

2. **Experimental section**

Starting materials for the synthesis of U$_3$Fe$_4$Ge$_4$ were uranium turnings (99.8 %), iron pieces (Strem, 99.999%), germanium (Strem, 99.999%). Calculated amounts of the components were melted under low pressure of argon, in an arc-furnace. In order to ensure a good homogeneity, the buttons were flipped and re-melted two times. Crystal growth was carried out with the help of a high frequency induction furnace, the sample was placed into a cold copper crucible under high vacuum. The sample was heated at 1700°C then slowly cooled down to 1000°C over 4 hours, and finally to room temperature after switching off the power. Single crystals were mechanically isolated from the heat-treated ingot.

Metallographic observations and elementary analyses were carried out with the help of a 6400-JSM scanning electron microscope equipped with an Oxford Link-Isis spectrometer. A piece, of each sample prepared for the present study, was embedded in resin and polished using SiC paper and diamond paste down to 1 μm. A thin layer of gold was deposited on the surface of the sample holder. X-ray powder diffraction patterns were recorded using an Inel CPS 120 diffractometer working with a Kα Co radiation. Single crystal X-ray diffraction experiments were performed on a Nonius Kappa CCD diffractometer working with a Kα Mo radiation. The unit-cell parameters, orientation matrix as well as the crystal quality were

derived from 10 frames recorded at $\chi = 0$ using a scan of 1° in ϕ. The complete strategy to fill more than a hemisphere was automatically calculated with the use of the program COLLECT [11]. Data reduction and reflection indexing were performed with the program DENZO of the Kappa CCD software package [11]. The scaling and merging of redundant measurements of the different data sets as well as the cell refinement was performed using DENZO. Semi-empirical absorption corrections were made with the use of the programs MULTISCAN [12]. Structure models were determined by direct methods using SIR-97 [13]. All structures refinements and Fourier syntheses were made with the help of SHELXL-97 [14]. The atomic positions were standardized with the help of STIDY [15]. The representations of the crystal structures were drawn with the help of DIAMOND 2.1 [16].

The electrical resistivity was measured in the temperature range 1.7-300 K temperature range using the four-probe AC method. The thermoelectric power was measured in a closed-cycle refrigerator in the temperature range 18-300K, relative to gold by a slow AC technique (10^{-2}Hz), with a thermal gradient of 1K, in a home-made apparatus similar to the one previously described by Chaikin et al. [17].

DC magnetic measurements were carried out using a Quantum Design MPMS-5 SQUID magnetometer. Data were collected in the temperature range 2 - 300 K with applied fields of 5 kOe. The magnetization was measured at 2K in increasing and decreasing magnetic fields up to 50 kOe.

3. Results

3.1 Sample preparation and Crystal structure refinement.

The systematic investigation of the U-Fe-Ge ternary system revealed the existence of this new compound. The synthesis of $U_3Fe_4Ge_4$ was undertaken by induction melting, by decreasing the temperature from the liquid (temperature of Liquidus estimated at about

1700°C) to 1000°C over 4 four. After the air-quenching, the sample appears as a dense, large-grain ingot from which a single crystal with a prismatic shape was extracted. Refinement of the crystal structure was carried out in the orthorhombic space group, *Immm* (n°71). Cycles of full-matrix least-squares calculation rapidly converged to a distribution of atoms similar to that reported for the $Gd_3Cu_4Ge_4$-type. Refinements of the structure showed no indication of any deviations from full occupancies of the U, Fe, or Ge sites. The main crystallographic details of the single crystal X-ray diffraction experiments are gathered in Table 1. Table 2 reports the positional and equivalent isotropic displacement parameters, and interatomic distances are listed in Table 3. Further details on the crystal structure investigations can be obtained from the Fachinformationszentrum Karlsruhe, 76344 Eggenstein-Leopoldshafen, Germany, (fax: (49) 7247 808 666; e-mail: crysdata@fiz.karlsruhe.de) on quoting the depository number CSD xxxxxx. Metallographic observations and powder X-ray diffraction experiments performed on pieces of the ingot, revealed a single phase sample, and a powder pattern which could be fully indexed with the orthorhombic $Gd_3Cu_4Ge_4$ type of structure.

3.2 Description of the crystal structure.

Despite a commonly adopted description of the structural arrangement of the $Gd_3Cu_4Ge_4$ type of structure based on a periodic intergrowth of ordered AIB_2 and ordered $BaA1_4$ segments, [18-20], a description using polyhedrons as been preferred for $U_3Fe_4Ge_4$ (Figure 1). Another striking feature of the $Gd_3Cu_4Ge_4$ type is the rather high symmetric arrangement about the *d* transition metal. Indeed, the Fe atoms in $U_3Fe_4Ge_4$ adopt a slightly distorted tetrahedral arrangement of Ge atoms with angle close to 109°. The average Fe-Ge distances of 2.50 Å points to strong bonding likely. The coordination sphere about Fe atoms is completed by 3 Fe at distances ranging from 2.651(2) to 3.009(8) and by 3 U atoms (U2) at distances of 2.908(8) and 2.968(6) (Figure 2.a). The FeGe4 tetrahedrons pack by face-sharing in the *b*-

direction and edge-sharing in the *c*-direction. The two inequivalent uranium atoms per unit-cell have high coordination sphere, composed of 4 Ge2, 2 Ge1 and 8 Fe1 for U1 and of 4 Ge2, 4 Ge1, 6 Fe1 and 1 U2 for U2. The six nearest germanium ligands of both uranium atoms form an elongated (along c) octahedron and a trigonal prism around U1 and U2, respectively. Theses U-Ge interatomic distances ranging from 2.889(7) to 3.023(8) Å, compare well the interatomic distances reported for binary uranium germanides [21, 22]. U1 is additionally coordinated by 8 Fe atoms in a rectangular prismatic geometry (Figure 2.b). The U1-Fe distances of 3.402(1) Å suggest weak interaction likely. Besides the trigonal prismatic environment of Ge ligands around U2, the central atom is bonded to 6 Fe atoms at distances ranging from 2.909(8) to 2.968(6) Å. These contacts compare well the U-Fe distances found for UFe_2 [23] and for other U-Fe-Ge ternary compounds [5, 6, 9]. The coordination sphere around U2 (Figure 2.c) is completed by 2 Ge1 atoms and 1 U2 atoms, which capped the rectangular faces of the trigonal prism, at much longer distances of 3.494(6) Å and 3.643(1) Å for Ge1 and U2, respectively. The trigonal prisms around U2 share rectangular faces in *c*-direction, and pack with octahedrons around U1 by corner-sharing along c, and edge-sharing in the *ab*-plane. Finally, the FeGe4 tetrahedral motifs condense with U1 octahedrons and U2 trigonal prim by face-sharing.

   The shortest U-U distances of 3.643(1) Å, resulting from the face-sharing of two trigonal prisms around U2, are larger than the Hill limit of 3.5 Å for U–U interactions [24].

   3.3 Electrical transport properties
   Figure 3 shows the temperature dependence of the electrical resistivity of $U_3Fe_4Ge_4$ measured in the temperature range 1.7-285K. The resistivity, first slightly decreases with decreasing temperature to reach an inflection point, below which it drops abruptly, indicating the onset of magnetic ordering at low temperature. Regarding, the resistivity at room

temperature of the order 3.8 μΩ.m and the low variation of $\rho(T)$ in the paramagnetic region, yet with a pronounced curvature, the compound is best classified as a semi-metal. In line, with this observation, the residual resistivity ratio RRR is about 8 for the specimen measured (large scale monodomains).

As shown in the left inset of Figure 3, the magnetic ordering manifests itself as a distinct peak in the temperature derivative of the resistivity, pointing to a precise value of 17(1)K for the magnetic phase transition. The fit of the data (right inset) using a simple Fermi liquid relation, $\rho(T) = \rho_0 + AT^2$, where ρ_0 is the residual resistivity at low temperature, was achievable for T < 14K, only. It yields the values ρ_0 = …. μΩ.m, and A = μΩ.m/K^2 suggesting, however, that the resistivity is dominated by electron-electron interactions at low temperature.

Figure 4 displays the thermal variation of the thermoelectric power of $U_3Fe_4Ge_4$. The Seebeck coefficient is rather small, being of the order of few μV/K in the whole domain of temperature. It continuously decreases with the decrease of the temperature, with an inflection in the slope at about 100K, suggesting a change in the mechanism of conduction. The thermoelectric power changes its sign from positive at high temperatures to negative below 90 K. For temperatures below 90K, $S(T)$ dependence is roughly linear indicating that the total thermopower is dominated by the contribution from thermal diffusion of carriers (electrons), whereas at higher temperatures, the non-linear temperature dependence of S(T) may suggests that phonon-drag interactions becomes dominant. The change in the slope itself, could be explained by the electron-phonon interaction renormalization effects. The authors are perfectly awarded that several scenarios may explain the change in the dominant mechanism of contribution to the total thermopower, but it can be reasonably attempted that two competing phenomena exist and likely compensate in the whole temperature domain yielding such low value of the Seebeck coefficient.

3.4 Magnetic behavior

Figure 5 present the magnetization of $U_3Fe_4Ge_4$ as a function of temperature measured in an applied field of 5 kOe. The curve is a characterized by a ferromagnetic-like transition at low temperature. The temperature dependencies of real and imaginary part of the Ac susceptibility recorded for a HAC amplitudes (10 Oe with f = 500 Hz − not shown) clearly indicate that the excepted magnetic transition occurs at 17(1)K, in agreement with the temperature of magnetic phase transition deduced from the resistivity curve. The easy rotation of the magnetic moments with the applied field is evidences on the magnetization curve at 2K (inset Figure 5), which shows a rapid increase at low applied fields (H < 2 kOe). For higher applied fields (H > 5kOe), the magnetization increases linearly without reaching saturation under 50 kOe. Finally the remanent magnetization at 2K amounts to 0.55(2) μ_B per formula unit. Despite the measurement was performed on a randomly oriented polycrystalline sample, such a value is quite low, considering a chemical formula of three U atoms and four Fe atoms per unit. It may originates from (i) an antiferromagnetic coupling of two independent magnetic sublattices (ferrimagnetism), (ii) the absence of magnetic moments on one or several atoms of the unit-cell, or (iii) a significant reduction of the ordered magnetic moments born by the U and Fe atoms, due to rather strong 3*d*-5*f* hybridization. [3, 25].

The inverse of the magnetic susceptibility $1/\chi(T)$ of $U_3Fe_4Ge_4$ plotted in the temperature range 2 - 350K is depicted on Figure 7. It is rather linear in the range of temperatures 150-350K, whereas it becomes strongly curvilinear in the domain 20-150K. The data were therefore fitted according to two models, a Curie-Weiss law, $\chi = \dfrac{C}{T - \theta p}$ in the linear portion of the curve and a modified Curie-Weiss law $\chi = \dfrac{C}{T - \theta p} + \chi_0$ over a wider range of temperature (35-350K). The fits yields the values of the Curie Constant, C = 18.5(2)

K.emu.mol^{-1} and the Weiss temperature, θp = -690(8)K for the linear portion (150-350K) and C = 0.89(2) K.emu.mol^{-1}, θp = 10(1)K and a Pauli independent term, χo = 1.57(1)10^{-2} emu.mol^{-1}, for the almost whole paramagnetic domain. For both cases, the derived Curie constants cannot be ascribed to any simple electronic model, however, the significant change of their values may reflect a change of the electronic structure, from a high temperature regime, in which the valence electrons are rather localized, to a low temperature regime in which these electrons appears to be more delocalized. At low temperature, the itinerant nature of the magnetic moments is evidenced by the T^2 decrease of the magnetization with temperature in the range 2-14K (Fig.5).

Mössbauer spectra taken at room temperature and at 4.2 K consist of a doublet that reflects the unique Fe atomic sites in the structure. The doublet absorption peaks (figure 6) can be fitted by a quadrupole doublet, with spectral parameters given in Table 4. No magnetic splitting is detected at 4.2 K. This indicates that neither the long-range magnetic ordering nor the standard spin-glass behavior of the iron sub-lattice is associated with the magnetic anomaly detected by magnetization measurements, suggesting that the magnetic ordering originates from the U atoms only.

4. Conclusion

In this present work, structural characterization and investigation of electronic properties of $U_3Fe_4Ge_4$ have been presented. Both transport and magnetic measurements reflect a change in the electronic structure of the compound as the function of temperature. At high temperature (150-350K), a rather localized system with a Curie-Weiss paramagnetic behaviour and a semi-metallic type of conduction is observed, whereas at low temperature (T < 150K) a more delocalized system, with the susceptibility best described with a modified Curie-Weiss law, and thermal dependence of the electrical resistivity featuring a metallic behaviour, shows up.

At lower temperature, $U_3Fe_4Ge_4$ undergoes to a magnetic phase transition below Tc = 17(1)K. In the temperature range 2-14K, both the resistivity and magnetization follow, T^2 relations indicating a Fermi-liquid behaviour and the itinerant nature of the magnetic state, respectively. The low value of both effective and ordered magnetic moments in the low temperature regime (2-150K), points rather strong $3d$-$5f$ hybridization [26], which may induced a significant reduction of the magnetic moments borne by the U and Fe atoms, up to the cancelation in the case of the Fe sublattice, as suggested by the Mossbauer spectra taken at 4.2K.

5.   Acknowledgement

6.   references

[1]   D. Aoki, A. Huxley, E. Ressouche, D. Braithwaite, J. Flouquet, J.P. Brison, E. Lhotel, C. Paulsen, Nature **413** (2001) 613.

[2]   N.T. Huy, A. Gasparini, D.E. de Nijs, Y. Huang, J.C.P. Klaasse, T. Gortenmulder, A. de Visser, A. Hamann, T. Görlach, H.v. Löhneysen, Phys. Rev. Lett., **99** (2007) 067006.

[3]   M.S.S. Brooks, O. Eriksson, B. Johansson, J.J.M. Franse, P.H. Frings, J. Phys. F, **18** (1988) L33.

[4]   D. Berthebaud, O. Tougait, M. Potel, E.B. Lopes, A.P. Gonçalves, H. Noël, *J. Solid State Chem.*, **180** (2007) 2926.

[5]   F.Canepa, P. Manfrinetti, M. Panni, A. Palenzona, *J. Alloys Compd.*, **234** (1996) 225.

[6]   R. Marazza, R. Ferro, G. Rambaldi, G. Zanicchi, J. Less- Common Met., **53** (1977) 193.

[7]   A.P. Gonçalves, J.C. Waerenborgh, G. Bonfait, M.M. Godinho, M. Almeida, J.C. Spirlet, *J. Alloys Compd.*, **204** (1994) 59.

[8]   T. Berlureau, B. Chevalier, L. Fournès, J. Etourneau, *Mater. Let.*, **9** (1989) 21.

[9]   M.S. Henriques, O.Tougait, H. Noël, L.C.J. Pereira, J.C. Waerenborgh, A.P Gonçalves, *Solid State Comm.*, **148** (2008) 159.

[10]   S.K. Dhar, K.V. Shah, P. Bonville, P. Manfrinetti, F. Wrubl, *Solid State Comm.*, **147** (2008) 217.

[11]   Nonius, In: Collect, Denzo, Scalepack, Sortav. Kappa CCD Program Package, Nonius BV, Delft, The Netherlands, 1998.

[12]   R. H. Blessing, *Acta Crystallogr.*, Sect A **51** (1995) 33.

[13]   A. Altomare, M.C. Burla, M. Camalli, G.L. Cascarano, C. Giacovazzo, A. Guagliardi, A.G.G. Moliterni, G. Polidori, R.J. Spagna, *J. Appl. Cryst.*, **32** (1999) 115.

[14]   G.M. Sheldrick, SHELXS97 and SHELXL97, Program for Structure Solution and Refinement: University of Göttingen, Germany. 1997.

[15]   E. Parthé, K. Censual, R. Gladyshevskii, *J. Alloys Compd.*, 197 (1993) 291.

[16]   W.T. Penningtona, DIAMOND - Visual Crystal Structure Information System, J. Appl. Cryst. 32 (1999) 1028.

[17]   P.M. Chaikin, J.F. Kwak, Rev. Sci. Instrum., 46 (1975) 218.

[18]   E. Hovestreydt, K Klepp, E. Parthè, *Acta Crystallogr*. Sect B., **38** (1982) 1803.

[19]   D. Kaczorowski, H. Noël, M. Potel, *Physica B*, **206-207**, (1995) 457.

[20]   S. Pechev, B. Chevalier, B. Darriet, P. Gravereau, J. Etourneau, *J. Alloys Compd.*, **243** (1996) 77.

[21]   P. Boulet, M. Potel, J. C. Levet, H. Noël, *J. Alloys Compd.,* **262-263**, (1997) 229.

[22]   P. Boulet, A. Daoudi, M. Potel, H. Noël, *J. Solid State Chem.*, **129**,, (1997) 113.

[23]   G. Katz, A.J. Jacobs, J. Nucl. Mater., 5 (1962) 338.

[24]   H.H. Hill, in: W.N. Miner (Ed.), Plutonium and Other Actinides, AIME, New York, 1970.

[25]   D.D Koeling, B.D. Dunlap, G.W. Crabtee, Phys. Rev. B, (1985) 31, 4966.

[26]   V. Sechovsky, L. Havela, in K.H.J. Buschow (Ed.), Handbook of Magnetic Materials, vol. 11, 1998, 1-289.

Table 1: Crystal data and structure refinements of U$_3$Fe$_4$Ge$_4$

Crystal label	
Empirical formula	U$_3$Fe$_4$Ge$_4$
Formula weight (g mol^{-1})	1227.9
Crystal system, space group	Orthorhombic, Immm (N°71)
Unit cell dimensions (Å)	a 4.090(5) b 6.639(5) c 13.702(5)
Volume (Å^3)	372.06(6)
Z, Calculated density (g/cm^3)	2, 10.96
Absorption coefficient (cm^{-1})	88.363
Crystal color	Black
Theta range for data collection (°)	5.2-45
Limiting indices	$-7 \leq h \leq 8$ $-13 \leq k \leq 12$ $-17 \leq l \leq 26$
Reflections collected/unique	5434/906
R(int)	0.08
Absorption correction	Semi-Empirical (MULTISCAN)
Refined parameters	23
Goodness-of-fit on F^2	1.106
wR$_2$ (I>2σ(I)])	0.063
R [I>2σ(I)]	0.031
Extinction coefficient	0.0035
Largest difference peak and hole (e Å^{-3})	-4.019/3.313

[a] R(F)=$\Sigma \, \|F_0| - |F_c\| / |F_0|$, ωR$_2$=[$\Sigma\omega(F_0^2 - F_c^2)^2/\omega F_0^4$]^{¼}, where ω^{-1}=[$\sigma^2(F_0^2)$+7.27P], P=[max(F_0^2,0) + 2F_c^2]/3

Table 2: Atomic coordinates and equivalent isotropic displacement parameters ($\mathring{A}^2$) for $U_3Fe_4Ge_4$

Atome	Position de Wyckoff	x	y	z	$U_{eq}(\mathring{A}^2)$
U(1)	2a	0	0	0	0.0132(8)
U(2)	4j	0.5	0	0.3670(4)	0.0119 (6)
Fe(1)	8l	0	0.3003(2)	0.3267(6)	0.0151(9)
Ge(1)	4i	0	0	0.2124(5)	0.0124(6)
Ge(2)	4g	0	0.1927(8)	0.5	0.0129(3)

Table 3: Interatomic distances (Å) for U$_3$Fe$_4$Ge$_4$

U1	4Ge2	2.888(8)	Fe1	1Ge2	2.479(4)	Ge2	2Fe1	2.479(4)
	2Ge1	2.911(1)		2Ge1	2.496(6)		1Ge2	2.560(2)
	8Fe1	3.402(1)		1Ge1	2.536(6)		2U1	2.888(8)
	4U2	3.787(8)		1Fe1	2.651(2)		4U2	3.023(9)
				2U2	2.909(8)			
				1U2	2.968(6)			
				2Fe1	3.009(8)			
U2	4Fe1	2.909(8)	Ge1	4Fe1	2.496(6)			
	2Ge1	2.944(8)		2Fe1	2.536(7)			
	2Fe1	2.968(6)		1U1	2.911(1)			
	4Ge2	3.023(9)		2U2	2.944(6)			
	2Ge1	3.494(6)		2U2	3.494(6)			
	1U2	3.643(1)						
	2U1	3.787(8)						

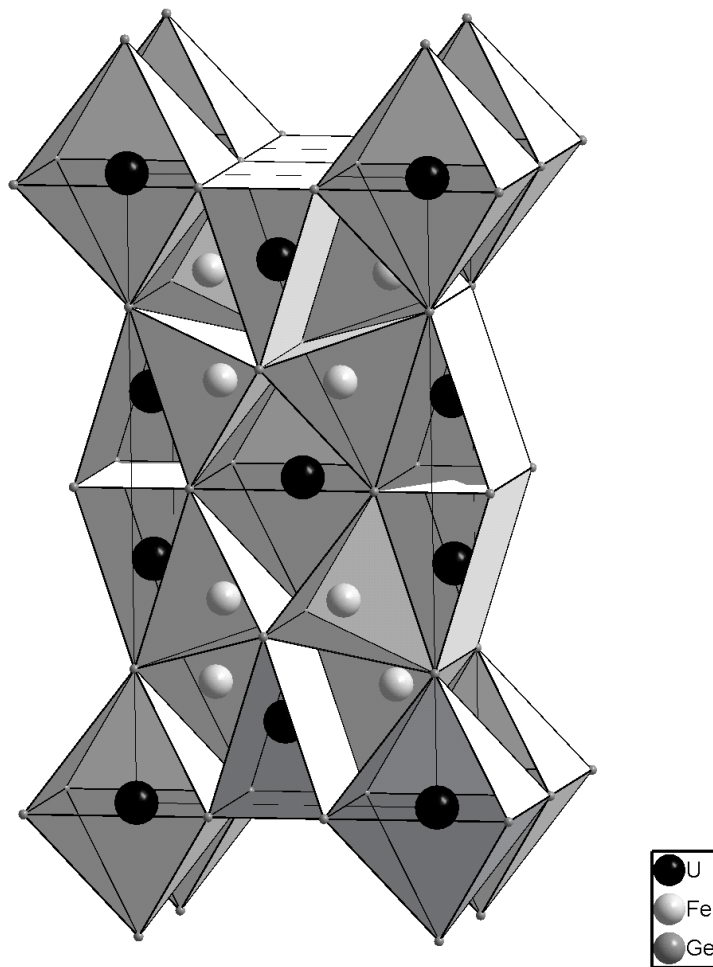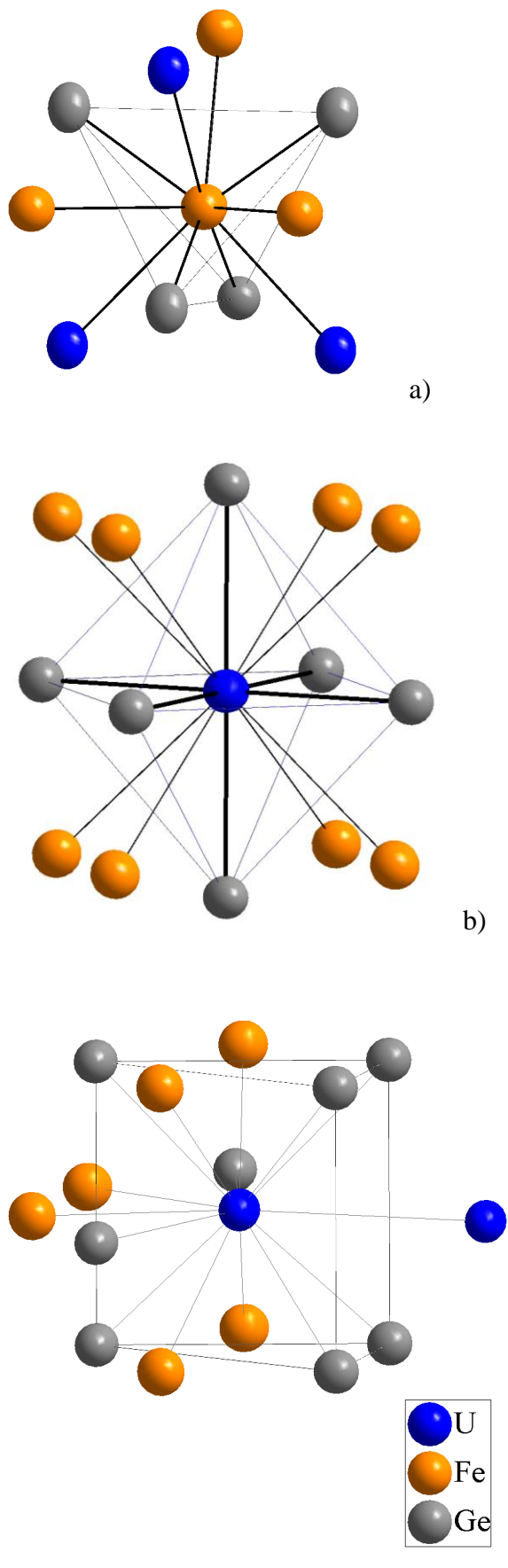**Figure 1: Polyhedral view of U$_3$Fe$_4$Ge$_4$. The black and grey sphere are U and Fe atoms, respectively.**

Figure 2. a, b, and c: Coordination polyhedrons around Fe (a), U1 (b) and U2 (c) atoms in U3Fe4Ge4.

a)

b)

	U
	Fe
	Ge

c)
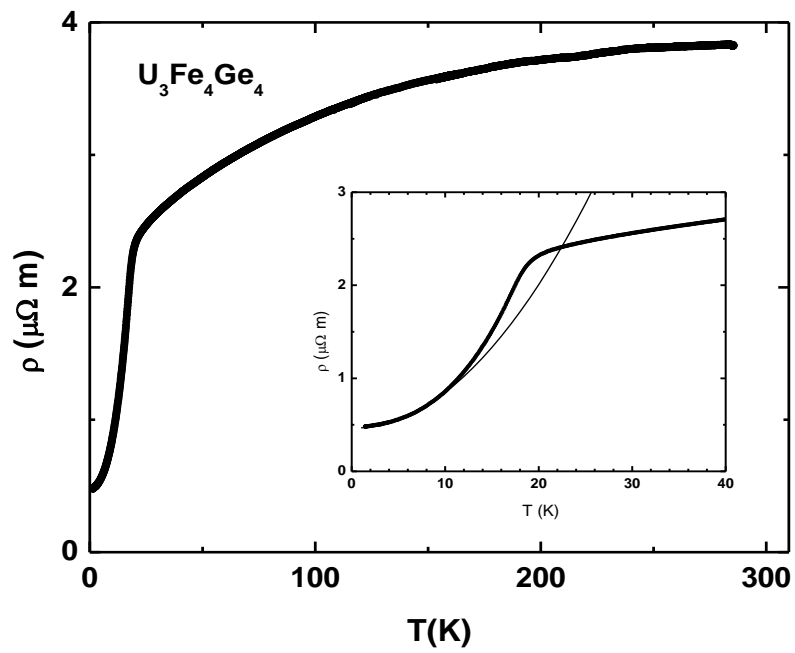
Figure 3 : Electrical resistivity of U₃Fe₄Ge₄ versus temperature

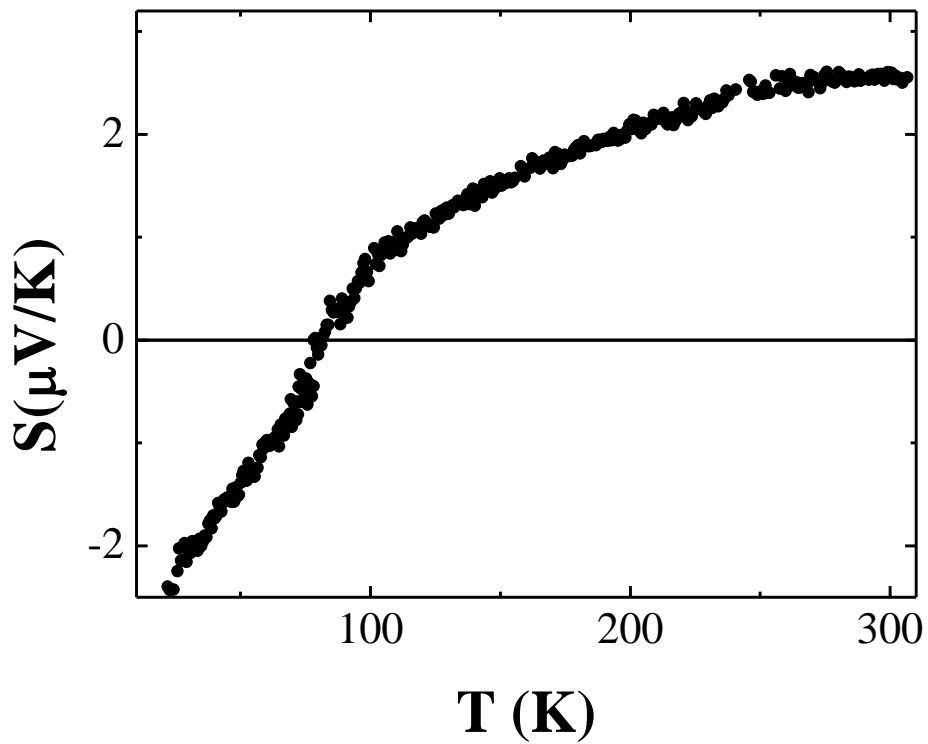**Figure 4 : Temperature dependence of Seebeck coefficient of U₃Fe₄Ge₄**

Figure 5: Temperature dependence of the magnetization divided by the applied field H of U$_3$Fe$_4$Ge$_4$ measured in Zero Field Cooled mode. The solid line represents the T^2 variation of magnetization in the temperature range 2-14K. The inset shows the magnetization of U$_3$Fe$_4$Ge$_4$ at 2K in applied filed up to 50 kOe.
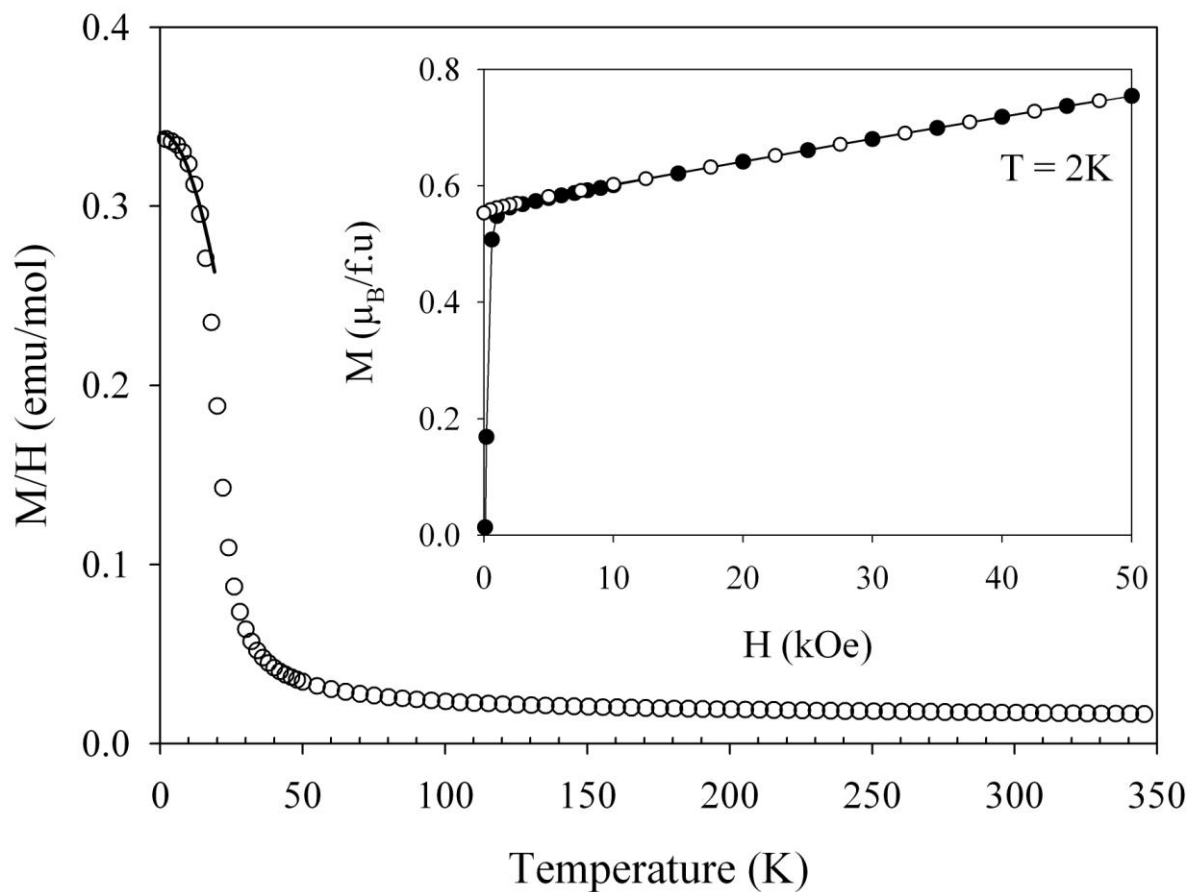
Figure 6: Thermal dependence of the inverse of susceptibility of U₃Fe₄Ge₄. The straight line in blue corresponds to the fit of the data by a Curie-Weiss law in the temperature domain 150-350K, whereas the curve in red represents the fit of the data by a modified Curie-weiss law in the temperature range 35-350K
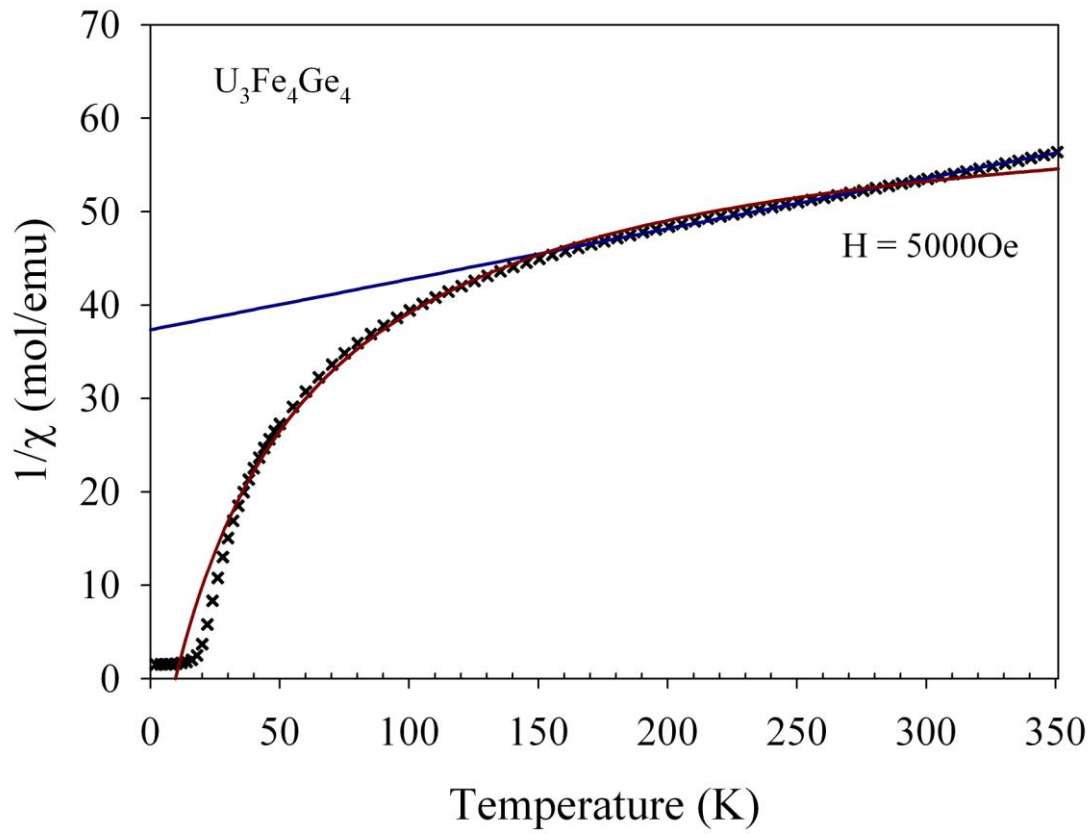
Figure 7 : ^{57}Fe Mossbauer spectrum of U$_3$Fe$_4$Ge$_4$